

Wind observations pertaining to current disruption and ballooning instability during substorms

Li-Jen Chen,¹ A. Bhattacharjee,¹ K. Sigsbee,² G. Parks,² M. Fillingim,² and R. Lin²

Received 21 September 2002; revised 20 January 2003; accepted 31 January 2003; published 28 March 2003.

[1] The westward propagation of wave disturbances associated with current disruption is observed in the near-Earth plasma sheet by the Wind satellite. By analyzing the time delay between earthward and tailward flux enhancements of energetic ions, the propagation velocity is estimated to be several hundred kilometers per second. A large anisotropy between the duskward and dawnward fluxes of energetic ions is observed to persist until the local onset of a current disruption. This anisotropy is consistent with an earthward density gradient which is significantly reduced after the magnetic fluctuations that accompany the current disruption cease. The reduction process is impulsive and bursty, suggesting that the underlying dynamics is nonlinear. The westward propagation of the unstable wave disturbances, the radial density gradient and its subsequent reduction support the drift ballooning instability as a possible mechanism for triggering substorms. **INDEX TERMS:** 2788 Magnetospheric Physics: Storms and substorms; 2744 Magnetospheric Physics: Magnetotail. **Citation:** Chen, L.-J., A. Bhattacharjee, K. Sigsbee, G. Parks, M. Fillingim, and R. Lin, Wind observations pertaining to current disruption and ballooning instability during substorms, *Geophys. Res. Lett.*, 30(6), 1335, doi:10.1029/2002GL016317, 2003.

1. Introduction

[2] What mechanism triggers magnetospheric substorms is still an open question. One mechanism that has been proposed is the drift ballooning instability [Roux *et al.*, 1991; Cheng and Lui, 1998; Lee, 1999; Zhu *et al.*, 2003]. The drift ballooning instability is driven by the plasma pressure gradient, and the wave perturbations to which the system is unstable propagate in the direction perpendicular to the pressure gradient and the background magnetic field. In the context of the magnetotail current sheet, the propagation occurs in the dawn-dusk (east-west) direction, in the same direction as the duskward ion diamagnetic drift [Zhu *et al.*, 2003]. The duskward propagation is a distinct auroral feature called the westward traveling surge which has been suggested to be the auroral signature of the drift ballooning instability in the equatorial region of the near-earth plasma sheet [Roux *et al.*, 1991].

[3] Substorm onsets are accompanied by abrupt changes in the magnetic field and enhancements in energetic particles in the near-earth plasma sheet [Takahashi *et al.*, 1987;

Ohtani *et al.*, 1992, and references therein]. The abrupt magnetic field changes have been interpreted as disruptions of the cross-tail current [Lui *et al.*, 1992]. Large variations in energetic particle fluxes and the initiations of large magnetic field fluctuations (a signature for local current reconfiguration, see Lui *et al.* [1992]) are coincident in time. Hence, it is possible to extract information on the propagation direction of the current disruption from energetic ion data owing to the large gyroradii. For example, time delays between duskward and dawnward flux variations observed at synchronous altitudes have been interpreted as the radial and north-south motion of particle boundaries [Walker *et al.*, 1976], and at AMPTE/CCE orbit ($\leq 8.8 R_E$) as the radial motion of the current disruption front [Ohtani *et al.*, 1992]. A similar technique has also been applied to determine the propagation properties of ULF waves [Lin *et al.*, 1988].

[4] In this paper, we deduce the westward propagation of the unstable wave associated with current disruption based on the time delay between earthward and tailward flux enhancements of energetic ions (~ 75 keV–1 MeV). This is the first time the westward propagation signature of current disruption is reported from the perspective of energetic ions. The time delay analysis on ion data does not have the spatial-temporal ambiguity that is inherent in the minimum variance analysis of the magnetic field data performed earlier [Roux *et al.*, 1991]. The full 3D particle [Lin *et al.*, 1995] and magnetic field [Lepping *et al.*, 1995] measurements can further substantiate the westward propagation of the magnetic field disturbances observed in the plasma sheet, thus providing additional evidence that the drift ballooning instability is a possible substorm trigger mechanism.

[5] Another critical feature of the drift ballooning instability is that the pressure gradient points in the same direction as the magnetic curvature. Near the equatorial plane, the magnetic curvature is toward the earth. Hence, an important question is whether an earthward pressure gradient is observed, and how the pressure gradient evolves during the course of the instability. The pressure gradient is proportional to the density gradient for isothermal plasmas. Observations of radial density gradients before breakups have been reported at the synchronous orbit based on Geos 2 data [Roux *et al.*, 1991], and at ~ 8 – $9 R_E$ using AMPTE/CCE data [Ohtani *et al.*, 2000]. The higher quality Wind data permits us to monitor with high time resolution the radial density gradient from ~ 5 minutes before the onset of a current disruption to ~ 5 minutes after the magnetic field fluctuations end.

2. Observation

[6] Two substorm onset events were selected including a pseudo-substorm event on July 26, 1997, when Wind was at GSE ($-10, 4, 0$) R_E and an isolated substorm event on

¹Center for Magnetic Reconnection Studies, Department of Physics and Astronomy, University of Iowa, Iowa City, Iowa, USA.

²Space Sciences Laboratory, University of California, Berkeley, California, USA.

October 4, 1996, when Wind was $(-8, -1, -0.5) R_E$. The first event has been studied extensively by *Fillingim et al.* [2000, 2001], and it was concluded that there is no difference in the plasma sheet signatures measured in situ for substorms and pseudo-substorms.

[7] A schematic diagram of the coordinate system and the key ideas involved in the interpretation is shown in Figure 1. The coordinate system is Geocentric Solar Ecliptic (GSE) with X toward the Earth, Y toward dusk, and Z the third direction for a right hand coordinate system. The squares in both Figures 1a and 1b denote the spacecraft. The diagram illustrates the simple case of a uniform magnetic field (\mathbf{B}) pointing in the Z direction, and ions gyrating clockwise on the XY plane. When a front of energetic ions (represented by a row of three circles with the gyration directions marked by arrows) propagating duskward encounters the spacecraft, the spacecraft first sees at time t the earthward flux enhancement, followed by the tailward flux enhancement at time $t + \tau$. Figure 1a illustrates this situation where τ is the time delay between earthward and tailward flux enhancements and is positive for duskward propagation. (A negative τ corresponds to dawnward propagation of the particle front and in this case the tailward flux enhancement would appear prior to the earthward enhancement.) The velocity of the particle front is $2 R_g/\tau$ duskward, where R_g is the gyroradius.

[8] Figure 1b illustrates how an anisotropy in duskward and dawnward fluxes can indicate a density gradient in the X direction. The ions going duskward (90°) at the spacecraft position have their guiding centers earthward of the spacecraft, while the ions going dawnward (270°) have guiding centers tailward of the spacecraft. Hence, a persistent dawn-dusk anisotropy is consistent with a stationary density gradient in the radial direction. This density gradient is the density gradient of energetic ions, and its time variation is representative of the time variation of the bulk ion density gradient provided that the ratio of energetic ion density to the bulk ion density does not vary much from one R_g earthward of the spacecraft to one R_g tailward of the spacecraft.

[9] For the first event, we use only measurements of the ions with energies above 100 keV for the time delay analysis, because ions with this high energy are not present in this region during quiet time and hence provide a clean signature for the current reconfiguration. The top five panels in Figure 2 plots the earthward (black trace, denoted as 0 on the right of the top panel) and tailward (green trace, denoted as 180) fluxes, panels 6–10 duskward (blue trace, denoted as

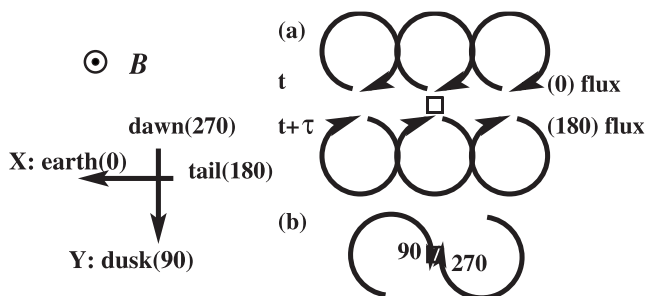


Figure 1. A schematic illustration of the coordinate system and how the large gyroradii of ions can enable the extraction of information about wave propagation and density gradients.

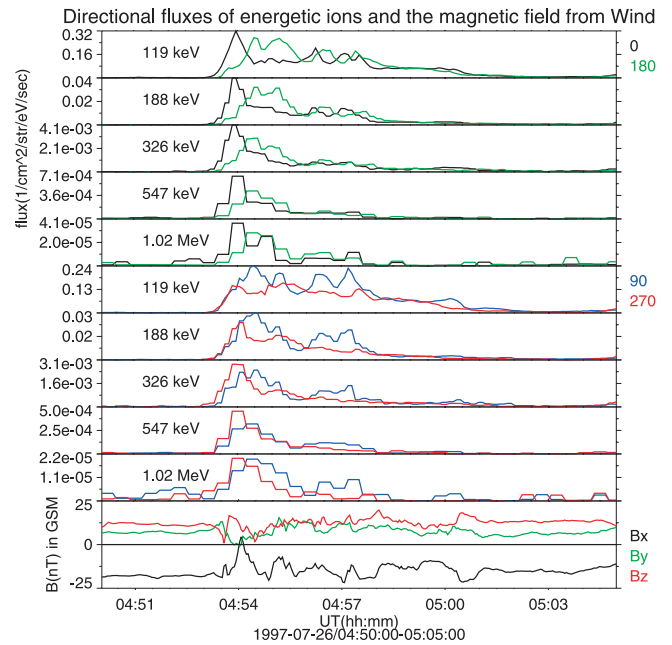


Figure 2. Directional flux enhancements of energetic ions and the three components of the magnetic field observed in the plasma sheet at the onset of a pseudobreakup. In the top five panels, the time delay between the earthward (black trace) and tailward (green trace) flux enhancements in each channel is a signature of westward propagation of the current disruption front. Panels 6–10 show the duskward (blue trace) and dawnward (red trace) fluxes.

90) and dawnward (red trace, denoted as 270) fluxes, and the bottom panel the three components of the magnetic field. In the top five panels, a sharp rise occurs in the earthward flux for ions with energies ~ 100 keV to 1 MeV, and abrupt excursions in B_x and B_z also occur at $\sim 04:53:30$ UT. An auroral pseudo breakup onsets at about the same time (see Figure 2 in *Fillingim et al.* [2001]). For all the five energy channels, the earthward fluxes reach their peaks at $\sim 04:54$ UT. The tailward flux enhancements have similar profiles as they rise sharply and fall gradually. There is a time delay between the earthward and tailward enhancements.

[10] To quantify the time delays, we carry out cross correlation analysis on the earthward-tailward flux profiles. The result yields a time delay of 24 ± 18 sec at 119 keV, 24 ± 18 sec at 188 keV, 24 ± 18 sec at 326 keV, 24 ± 24 sec at 547 keV, and 24 ± 24 sec at 1.02 MeV. The time delay for each energy channel is the time shift between the two flux enhancements that yields the peak correlation coefficient. The error bars are obtained by taking into account the instrument time resolution and the different pulse shapes. With these time delays and a B_z of strength 10 nT, we obtain the guiding center velocity that is consistent with the measurements for all energy channels to be 440 ± 250 km/s. This velocity is also the propagation velocity of the unstable wave perturbation, assuming that the ion guiding centers are carried along by the wave disturbance.

[11] The overall profiles for the duskward and dawnward enhancements also have sudden rises and gradual falls, but there are no pronounced time delays. We interpret the lack of time delays as evidence that the current disruption front, where it encounters the spacecraft, has no detectable struc-

ture in the X direction, that is, uniform in X for a scale of at least two ion gyroradii (such as the configuration drawn in Figure 1a). This feature is consistent with the ballooning ordering $k_y \gg k_x$, where k_y and k_x are the wave numbers in the dawn-dusk and radial directions respectively.

[12] The second event is an isolated substorm as recorded by the high latitude ground magnetometer stations (data not shown). The top four panels of Figure 3 present the earthward and tailward flux profiles, the next four panels the westward and eastward profiles, and the bottom panel the magnetic field. Here we include the 75 keV channel to provide more information on the density gradient, and we do not include the 547 keV and MeV channels due to the low signal to noise ratios. This region is populated by energetic ions even before the onset of current disruption, which can be verified by comparing the flux levels with those for the previous event. There is no discernable density gradient in the dawn-dusk direction prior and after the current reconfiguration, as the earthward and tailward fluxes do not show an anisotropy. The fluxes are modulated by the fluctuating magnetic field, and there is a phase shift between the earthward and tailward flux variations. From the time delays between the flux peaks, we obtain a propagation velocity of the unstable wave associated with current disruption to be 180 ± 30 km/s toward dusk (westward).

[13] A persistent flux anisotropy is observed in the duskward and dawnward fluxes. This is consistent with a quasi-stationary density gradient with higher density earthward of the spacecraft. Such a configuration would produce a duskward ion diamagnetic drift which is consistent with the duskward propagation deduced from the time delay analysis. From the ratio of the duskward to dawnward fluxes, we can also obtain a characteristic scale length L of the density gradient for each energy channel by

$$L = \frac{n}{\nabla n} \sim \frac{2R_g}{\text{flux ratio}}.$$

The resulting characteristic scale length ranges from ~ 1600 to 3400 km. This scale length combined with the measured temperature (2.7 keV, not shown) and the magnetic field (15 nT, in the \hat{z} direction) yields an ion drift velocity ~ 90 km/s duskward, consistent with the duskward propagation velocity obtained from the time delay analysis within a factor of 2. This good agreement shows that L obtained from energetic ion measurements is representative of the characteristic scale length of the bulk ion density gradient.

[14] B_z is the dominant component in this case, and oscillations of amplitudes a few nT start at 14:06 UT and last for ~ 40 seconds. Thereafter B_z rises sharply for ~ 15 nT in one cyclotron period (3 seconds), and large excursions occur with $\delta B/B$ exceeding 1. These variations seem to form a tripolar pulse structure that marks the onset of large fluctuations, and this tripolar structure is repeated after ~ 80 seconds. Two other smaller tripolar pulses with similar widths appear consecutively in a nearly equal interval of time. There are two corresponding prominent peaks in ion fluxes. The spatial extent of the tripolar pulses has to be over $1 R_E$ to modulate the flux of 326 keV ions. As we can see in Figure 1a, the satellite samples the magnetic field along its trajectory, while the ions experience the local magnetic field along their cyclotron orbit. If the tripolar pulses do not have spatial extent over twice the gyroradius

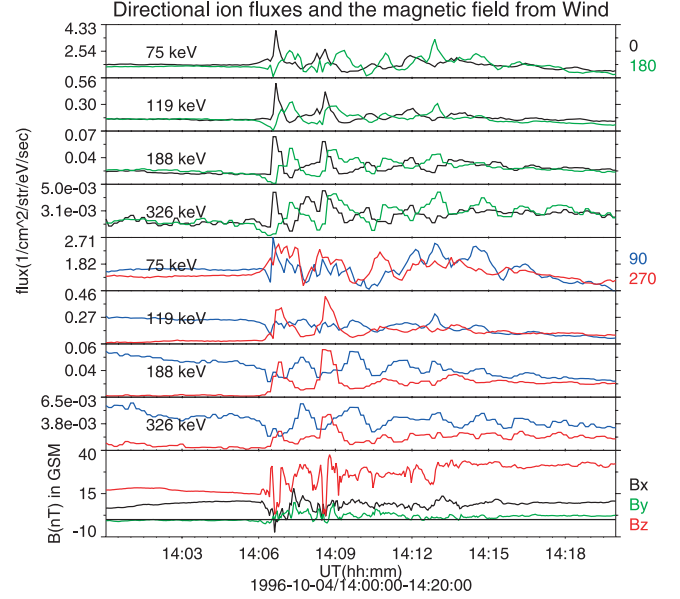


Figure 3. Energetic ion fluxes and the magnetic field observed in the plasma sheet ($\sim 8 R_E$). The format is similar to Figure 2. The start of large magnetic fluctuations and the modulation of ion fluxes coincide with the onset of an isolated substorm. Note the impulsive reduction of the anisotropy in the dawn-dusk fluxes.

of 326 keV ions, there would not be modulations in the four directional fluxes. After the magnetic field fluctuations cease, around 14:16 UT, the difference in dawnward and duskward fluxes has reduced to zero for 119 keV ions and to less than 50% for the 188 and 326 keV ions. Note that the reduction is through an impulsive process, and it actually overshoots (the anisotropy flips sign). The impulsive density gradient reduction and the overshoot are features beyond the scope of linear ballooning instability theories.

[15] An analysis of the magnetic disturbances measured in between the periods of the quasi-stationary radial density gradient and the relaxed state is carried out to obtain information about the instability that relaxes the density gradient. The result of a wavelet analysis is displayed in Figure 4. There is enhanced wave power in the drift ballooning frequency range. Another band of enhanced wave power lies at frequencies around 0.1 Hz, extending up to the Nyquist frequency for the 3 second data that we used. This higher frequency band appears to be bursty (the enhanced power turns on and off in a time scale comparable to the gyroperiod of ions), indicating breakdown of the exponential growth predicted by linear theories. The wave perturbation has a significant compressional component, since B_z is the dominating component, and most perturbations are in the B_z component.

3. Summary and Discussion

[16] In this paper, strong evidence is given for the westward propagation of wave disturbances associated with current disruption in the tail plasma sheet at radial distances 8 and $10 R_E$. The propagation speeds are estimated to be several hundred km/s based on the analysis of time delays between the earthward and tailward energetic ion flux

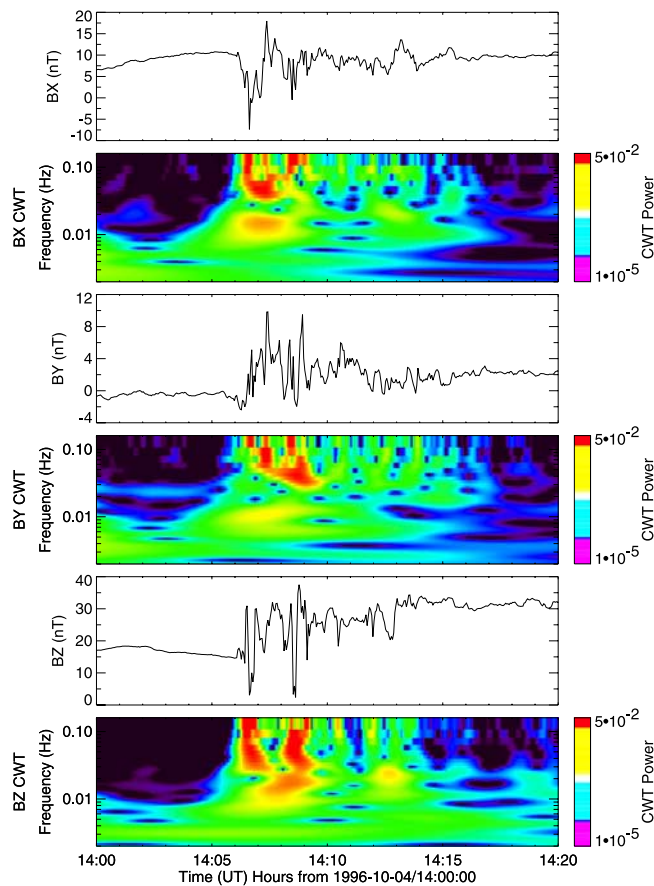


Figure 4. The power spectrograms for the three components of the magnetic field.

enhancements. Events with clear signatures of westward propagation (time delays between earthward and tailward flux enhancements) are not rare in the Wind data set. A preliminary survey shows that the occurrence rate is much higher for radial distances $\leq 10 R_E$, which suggests that the initially unstable region is localized at these near-Earth distances.

[17] A radial density gradient is observed to persist until the abrupt magnetic field changes, and the density gradient is reduced after the magnetic field recovers from the fluctuations. We have shown a complete time history of the density gradient including its impulsive reduction. We have monitored the density-gradient reduction process in action using probes of different scale lengths (ions with different gyroradii), and showed that the impulsive reduction occurs at the same time as the largest magnetic fluctuations. We were also able to deduce the scale size of the largest magnetic fluctuations to be at least $\sim 1 R_E$ (twice the gyroradii of the highest energy channel whose fluxes are modulated by the magnetic fluctuations). The instability that triggers the current disruption, and hence the substorm, has to be able to relax the radial pressure gradient (proportional to the density gradient for an isothermal plasma). This leads us to conclude that the ballooning instability is active.

[18] The power spectrogram of the highly fluctuating magnetic field observed during the reduction of the density gradient reveals broadband and bursty features, consistent with previous analysis of magnetic fluctuations associated

with current disruptions [Lui and Najmi, 1997; Sigsbee et al., 2002]. The large fluctuations ($\delta B/B \approx 1$), the broad-band and bursty features of the magnetic field indicate that the involved process is nonlinear. The enhancement of wave power in the ballooning frequency range agrees with earlier results [Holter et al., 1995; Perraut et al., 2000]. However, our conclusion is different from that of Perraut et al. who invoked another mechanism to trigger substorms because the power enhancement could not be explained by the exponential growth predicted by linear ballooning instability theories. We conclude that the signature of the westward propagation, the radial density gradient and its subsequent reduction, and the wave power enhancement in the ballooning frequency range support the drift ballooning instability as a possible mechanism for triggering substorms. However, a nonlinear theory is required to account for the observed signatures.

[19] **Acknowledgments.** Research at the University of Iowa is supported by NSF Grant No. ATM 00-0203 and the DOE Cooperative Agreement No. DE-FC02-01ER54651, and at the University of California at Berkeley by NASA Grant Nos. NAG5-10428 and NAG5-11804.

References

- Cheng, C. Z., and A. T. Y. Lui, Kinetic ballooning instability for substorm onset and current disruption observed by AMPTE/CCE, *Geophys. Res. Lett.*, **25**, 4091, 1998.
- Fillingim, M. O., G. K. Parks, L. J. Chen, M. Brittnacher, G. A. Germany, J. F. Spann, D. Larson, and R. P. Lin, Coincident POLAR/UVI and WIND observations of pseudobreakups, *Geophys. Res. Lett.*, **27**, 1379, 2000.
- Fillingim, M. O., et al., Comparison of plasma sheet dynamics during pseudobreakups and expansive aurorae, *Phys. Plasmas*, **8**, 1127, 2001.
- Holter, O., C. Altman, A. Roux, S. Perraut, A. Pedersen, H. Pécseli, B. Lybekk, J. Trulsen, A. Korth, and G. Kremser, Characterization of low frequency oscillations at substorm breakup, *J. Geophys. Res.*, **100**, 19,109, 1995.
- Lee, D.-Y., Stability analysis of the plasma sheet using Hall magnetohydrodynamics, *J. Geophys. Res.*, **104**, 19,993, 1999.
- Lepping, R. P., et al., The Wind magnetic field investigation, *Space Sci. Rev.*, **71**, 207, 1995.
- Lin, N., et al., Multi-point measurements of ULF wave phases using a multi-channel energetic ion detector, *Adv. Space Res.*, **8**, 437, 1988.
- Lin, R. P., et al., A three-dimensional plasma and energetic particle investigation for the Wind spacecraft, *Space Sci. Rev.*, **71**, 125, 1995.
- Lui, A. T. Y., and A.-H. Najmi, Time-frequency decomposition of signals in a current disruption event, *Geophys. Res. Lett.*, **24**, 3157, 1997.
- Lui, A. T. Y., et al., Current disruptions in the near-Earth neutral sheet region, *J. Geophys. Res.*, **97**, 1461, 1992.
- Ohtani, S., et al., Initial signatures of magnetic field and energetic particle fluxes at tail reconfiguration: Explosive growth phase, *J. Geophys. Res.*, **97**, 19,311, 1992.
- Ohtani, S., et al., Ion dynamics and tail current intensification prior to dipolarization: The June 1, 1985, event, *J. Geophys. Res.*, **105**, 25,233, 2000.
- Perraut, S., et al., Disruption of parallel current at substorm breakup, *Geophys. Res. Lett.*, **27**, 4041, 2000.
- Roux, A., et al., Plasma sheet instability related to the westward traveling surge, *J. Geophys. Res.*, **96**, 17,697, 1991.
- Sigsbee, K., et al., Geotail observations of low-frequency waves and high-speed earthward flows during substorm onsets in the near magnetotail from 10 to 13 R_E , *J. Geophys. Res.*, **107**(A7), 1141, 10.1029/2001JA000166, 2002.
- Takahashi, K., et al., Disruption of the magnetotail current sheet observed by AMPTE/CCE, *Geophys. Res. Lett.*, **14**, 1019, 1987.
- Walker, R. J., et al., Substorm-associated particle boundary motion at synchronous orbit, *J. Geophys. Res.*, **81**, 5541, 1976.
- Zhu, P., et al., Hall MHD ballooning instability in the magnetotail, *Phys. Plasmas*, **10**, 249, 2003.

A. Bhattacharjee, L.-J. Chen, and K. Sigsbee, Center for Magnetic Reconnection Studies, Department of Physics and Astronomy, University of Iowa, Iowa City, IA 52242, USA. (li-jen-chen@uiowa.edu)

M. Fillingim, R. Lin, and G. Parks, Space Sciences Laboratory, University of California, Berkeley, CA 94720, USA.